

Effects of ultrasound-assisted vacuum tumbling on the oxidation and physicochemical properties of pork myofibrillar proteins

Ruyu Zhang^a, Lujuan Xing^a, Dacheng Kang^b, Lei Zhou^a, Lin Wang^a, Wangang Zhang^{a,*}

^a Key Laboratory of Meat Processing and Quality Control, Jiangsu Synergetic Innovation Center of Meat Processing and Quality Control, College of Food Science and Technology, Nanjing Agricultural University, Nanjing, Jiangsu 210095, China

^b School of Life Sciences, Linyi University, Linyi, Shandong 276012, China

ARTICLE INFO

Keywords:

Ultrasound assisted-vacuum tumbling
Myofibrillar proteins
Protein oxidation
Protein structure
Physicochemical properties

ABSTRACT

The present research aimed to investigate the effects of high-intensity ultrasound (HIU, 20 kHz, 0 W, 100 W, 300 W and 500 W)-assisted vacuum tumbling (UVT) for 60 min and 120 min on the oxidation and physicochemical properties of the pork myofibrillar proteins (MPs). Compared with the vacuum tumbling (VT) groups without the HIU assistance, the carbonyl content increased, while the total sulfhydryl (SH) content was reduced with the increase of HIU power and treatment time ($P < 0.05$). The reactive SH content was increased significantly after treated by UVT with 300 W compared with the VT group ($P < 0.05$) regardless of the treatment time. Similarly, the surface hydrophobicity (S_0), the intrinsic tryptophan intensity, and the solubility in the UVT group (300 W) were remarkably higher than those of the VT group ($P < 0.05$). In contrast, the α -helix content and the particle size of MPs significantly decreased when the HIU power was at 100 W and 300 W ($P < 0.05$). The results suggest that UVT treatment could change the structure and physicochemical properties of MPs accompanied by protein oxidation.

1. Introduction

As a green and efficient technique, high-intensity ultrasound (HIU) is defined as the low ultrasonic frequency (20–100 kHz) with high ultrasonic intensity (10–1000 W/cm²) [1]. In a liquid medium, the sound wave of HIU could cause the growth and the collapse of vapor bubbles and thus generate cavitation [2,3]. During food brining, the cavitation could destroy the microstructure of food, which in turn accelerates the brining process [4,5]. Protein is an important component of the food matrix [6], and the physicochemical properties of protein largely determine the quality of food products. Many researchers have proved that HIU could positively modify the physicochemical properties of food proteins. Jiang et al. [7] reported that ultrasonic waves significantly contributed to unfolding the black-bean protein structure and caused the secondary structure to be flexible. Amir et al. [8] also found that the turbulence from cavitation could increase the exposure of the active regions and improve the solubility, the emulsifying properties, and the gel strength of myofibrillar proteins (MPs).

Tumbling exerts the mechanical force to roll the meat through the rotation of paddles or drums and is widely used in food product

processing [9]. Krause et al. [10] indicated that tumbling treatment could destroy the meat tissue, stimulate the brine diffusion into muscle, and further enhance the tenderness, juiciness and palatability of the cured meat product. Besides, vacuum tumbling (VT), as the specific tumbling mode, could result in negative pressure in the inner cavity of the drum. Marriott et al. [11] proved that vacuum tumbling boosted the brine transformation and kept the stable color of dry-cured ham. Similarly, Chen et al. [12] observed that by applying the vacuum tumbling (-0.06 MPa, totally 8 h) during curing duck meat samples, the actomyosin dissociation increased compared to the samples cured by static brining and pulsed pressure salting. Even though vacuum tumbling is widely applied to pre-treating the meat in the modern meat industry [13], the traditional single vacuum tumbling treatment still consumes time in the practical process, particularly for large meat pieces [14]. Moreover, no published studies have focused on the usage of HIU in combination with vacuum tumbling and its impacts on the physicochemical properties of MPs. Therefore, our work aimed to evaluate the effects of UVT treatment on the protein oxidation and the physicochemical properties of MPs with measuring the content of carbonyl and sulfhydryl (SH) groups, the secondary and tertiary structure, the particle

* Corresponding author at: National Center of Meat Quality and Safety Control, College of Food Science and Technology, Nanjing Agricultural University, Nanjing, Jiangsu 210095, China.

E-mail address: wangang.zhang@njau.edu.cn (W. Zhang).

<https://doi.org/10.1016/j.ultsonch.2021.105582>

Received 31 March 2021; Received in revised form 24 April 2021; Accepted 2 May 2021

Available online 4 May 2021

1350-4177/© 2021 The Authors.

Published by Elsevier B.V. This is an open access article under the CC BY-NC-ND license

(<http://creativecommons.org/licenses/by-nc-nd/4.0/>).

size, and the solubility of MPs.

2. Materials and methods

2.1. Sample preparation

Pork leg meat (*mesoglutaeus*) with the pH range of 5.6 to 5.8 was collected from Sushi Meat Processing Company (Huai'an, Jiangsu province, China) at 24 h of slaughter. All the visible fat and connective tissue of meat samples were trimmed. Then, these lean meat samples were cut with the size of $100 \times 40 \times 40 \text{ mm}^3$ with the weight of $200 \pm 5 \text{ g}$ and placed at $-20 \text{ }^\circ\text{C}$ after being vacuum-packaged.

2.2. Tumbling process

The ratio of brine and meat samples was set as 35:100 (v/w). The brine contained 3% NaCl and 0.3% composite sodium phosphates (the adding percentage referred to the weight of additive in relation to the weight of meat). The formulated brine was cooled at $4 \text{ }^\circ\text{C}$ before usage.

The UVT equipment in the study was mainly composed of a tumbling system, a HIU system and a temperature control system, which could ensure vacuum tumbling and HIU work simultaneously at a preset temperature (Fig. 1). The VT treatment was used as the control group. Meat samples and brine were put into the tumbler drum together. The tumbling time was set as 60 min and 120 min respectively (a cycle of 20 min work and 10 min rest). The working temperature was $4 \text{ }^\circ\text{C}$, the rotation speed was 10 rpm, the applied vacuum pressure was -0.08 MPa , and the angle between the tumbler and the ground was 35° . For UVT treatment, the tumbling parameters were the same as the VT treatment, and the HIU was set to be turned on or off synchronously according to whether the tumbling unit worked or not. HIU power was fixed at 100 W, 300 W and 500 W, respectively. Each treatment was replicated 4 times.

2.3. MPs extraction

MPs were prepared from meat samples after the tumbling process following the method of Han et al. [15]. Briefly, the meat samples were homogenized at 10,000 rpm with 4 volumes (w/v) of precooled buffer A (0.1 M KCl, 1 mM EGTA, 20 mM K_2HPO_4 , 2 mM MgCl_2 , 20 mM KH_2PO_4 , pH 7.0). The mixture was centrifuged at $2,000 \times g$ and $4 \text{ }^\circ\text{C}$ for 15 min (Beckman Avanti J-E, Beckman Coulter, Fullerton, CA, USA). After pouring the supernatant, the procedures were repeated twice using buffer A. Then, the precipitate was clarified twice with 4 volumes (w/v)

of buffer B (0.1 M NaCl). The clean precipitates were filtered with single gauze to discard connective tissues before the last time of centrifugation, and the pellets were collected. All the above processes were kept in an ice box. Finally, MPs pellets were dissolved in buffer C (0.6 M NaCl, 20 mM K_2HPO_4 , 20 mM KH_2PO_4 , pH 7.0) for further analysis. The protein concentration was measured by the Biuret method [16].

2.4. Carbonyl content

The carbonyl content was determined by adopting the method of Li et al. [17] with proper change. Accurately, the 1 mL protein suspension was diluted by the buffer C and mixed with 4 mL of 2,4 dinitrophenyl hydrazine (DNPH) and incubated at $25 \text{ }^\circ\text{C}$ for 30 min after vortexed for 60 s. Furtherly, 5 mL of 20% trichloroacetic acid (TCA) was added to stop the reaction, and then the samples were centrifuged at $12,000 \times g$ for 5 min ($4 \text{ }^\circ\text{C}$). The precipitation was washed three times by using 4 mL ethanol: ethyl acetate (1:1, v/v). Subsequently, the pellets were dissolved in 2 mL guanidine hydrochloride (6 M) and incubated at $4 \text{ }^\circ\text{C}$ overnight. Afterward, the absorbance of the supernatant obtained from centrifugation was tested at 370 nm (NanoDrop Technologies, Rockland, DE). The carbonyl content was calculated via the absorption coefficient of $22,000 \text{ M}^{-1}\text{cm}^{-1}$, and the carbonyl content was analyzed as nmol mg/protein.

2.5. SH content

The 500 μL MPs solutions (1 mg/mL) were mixed with 4.5 mL buffer (8 M urea, 10 mM EDTA, pH 6.0). The reaction was then conducted at $40 \text{ }^\circ\text{C}$ for 25 min avoiding light after adding 100 μL Ellman's reagent (0.1 M KH_2PO_4 buffer containing 10 mM DTNB, pH 6.0). For determining the contents of the reactive SH group, 4 mL MPs solutions (1 mg/mL) were mixed with 100 μL Ellman's reagent, and the mixture was placed at $4 \text{ }^\circ\text{C}$ for 1 h. The solution was immediately read at 412 nm, and the absorbance was used to calculate the SH groups by the extinction coefficient of $13,600 \text{ M}^{-1}\text{cm}^{-1}$ [18].

2.6. MPs secondary structure

MPs secondary structure of was measured by Raman spectrometer (Horiba Jobi Yvon S.A.S., Longjumeau, France). MPs pellets extracted from section 2.3 were put on a quartz slide, and the spectra of the secondary structure under the emit wavelength with 532 nm were collected. The ranges of measure spectra were $400\text{--}3,600 \text{ cm}^{-1}$ with three scans and an exposure time of 60 s. The objective lenses of the microscope were $50 \times$. The contents of 4 types of secondary structures were figured out using Peak Fit 4.12 software (Sea Solve Software Inc., San Jose, CA, USA) as mentioned by Zhou et al. [19].

2.7. MPs tertiary structure

2.7.1. Surface hydrophobicity (S_0)

The method of fluorescence probe (1-anilino-8-naphthalene-sulfonate, ANS) was used for determining the S_0 . Accurately, 20 μL ANS buffers (8 mM ANS, 10 mM KH_2PO_4) were added to 4 mL MPs solution (1 mg/mL). The mixtures were kept at $25 \text{ }^\circ\text{C}$ in the dark for 25 min after being thoroughly vortexed. Fluorescence intensity was measured at emissions from 410 to 570 nm with the excitation wavelength at 370 nm [20].

2.7.2. Intrinsic tryptophan intensity

MPs solution (1 mg/mL) was read at an excitation wavelength of 295 nm and an emission wavelength in the range of 300 to 400 nm according to the description of Zou et al. [21].

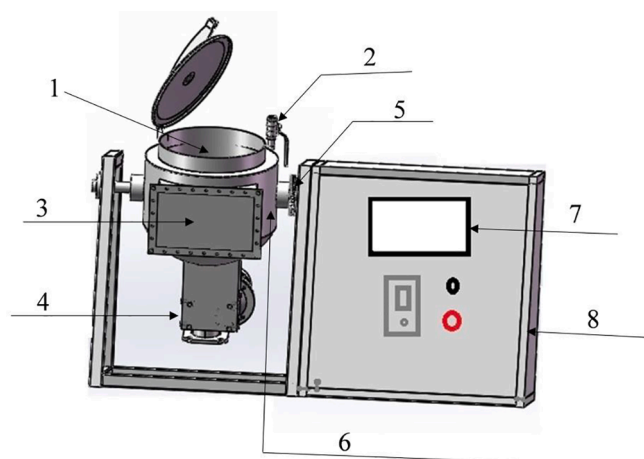


Fig. 1. Schematic diagram of the experimental ultrasound-assisted tumbling apparatus. 1. Tumbler drum; 2. Vacuum valve; 3. Ultrasonic transducer box; 4. Agitator motor; 5. Angle adjusting gear; 6. Coolant circulation interlayer; 7. Display screen; 8. Electrical control cabinet.

2.8. Particle size analysis

The particle size of MPs solution (1 mg/mL) was measured using a Mastersizer 3000 (Malvern Instruments Ltd., UK), and the D_{50} obtained by the Malvern SOP software was regarded as the average size.

2.9. MPs solubility

MPs solubility was determined by the centrifugation method following Dong et al. [22]. Briefly, 5 mL of 2 mg/mL MPs solutions were centrifuged at $10,000 \times g$ for 10 min at 4 °C. Protein solubility was calculated by the percentage of supernatant protein concentration compared to the initial suspension protein concentration [16].

2.10. Statistical analysis

The significance between different treatments was analyzed using SAS 9.2 for Windows. Fisher's LSD (Least Significant Difference) was selected by Bonferroni correction for analyzing the factors including HIU power, treatment time and their interaction. The differences in the results were regarded as significant when $P < 0.05$.

3. Results and discussion

3.1. Carbonyl content

Carbonyl derivatives could be readily formed after proteins are attacked by hydroxyl radicals, and the carbonyl content can be employed to assess the level of protein oxidation [23]. According to Table 1, the carbonyl content was significantly affected by the HIU power, the treatment time and their interaction ($P < 0.05$). No evident changes were observed in the VT group when the treatment time increased from 60 min to 120 min ($P > 0.05$). However, the carbonyl content of all UVT groups tended to increase along with the HIU power and treatment time and reached a maximum at HIU power of 500 W for 120 min ($P < 0.05$). This phenomenon indicates that UVT treatment induced protein oxidation, and it might attribute to the fact that the ultrasonic cavitation can produce highly reactive free radicals ($\cdot H + \cdot OH$) by the sonolysis of H_2O molecules [24], which can oxidize susceptible amino acid residues. Previous research by Kang et al. [25] has reported similar results which showed that a significant increase in the carbonyl content of beef samples after being sonicated by high HIU intensities ($>2.39 W/cm^2$, 20 kHz).

3.2. SH content

Table 1 also shows the total and reactive SH content in different

treatment groups at various treatment time. As for the total SH content, it was significantly affected by the HIU power, the treatment time and their interaction ($P < 0.05$). Compared to the VT group, the total SH content of all UVT groups had downtrends with the increase of treatment time and HIU power. Nevertheless, a significant reduction could be observed only when HIU power was higher than 300 W at each treatment time ($P < 0.05$).

On the other hand, regarding the reactive SH content (Table 1), it was greatly influenced by the HIU power, treatment time and the interaction of HIU power and treatment time ($P < 0.05$). Compared with the VT treatment, an upward trend could be observed in the reactive SH content after moderate HIU powers were used (100 W and 300 W). The reactive SH contents of the UVT groups at 100 W and 300 W were higher than that of the VT group at 120 min ($P < 0.05$). However, when meat samples were subjected to higher UVT treatment (500 W), the reactive SH content was significantly reduced in comparison with the UVT group of 300 W at each treatment time ($P < 0.05$).

The reactive SH refers to the SH groups distributed on the surface of the protein network, while the total SH refers to the SH groups spread both inside and surface of the protein network [8]. The previous studies have reported that hydroxyl radicals generated by ultrasonic cavitation were responsible for oxidizing the highly susceptible SH groups and caused a reduction of total SH content [25–27]. Therefore, in the present study, it could be speculated that the decrease in the total SH content possibly resulted from the formation of S-S bonds.

The increased reactive SH content suggested that the moderate power of UVT (100 W and 300 W) treatment could cause the MPs structure to unfold and expose the buried SH groups to the surface of the proteins [26]. Interestingly, as mentioned above, the reactive SH content was reduced when higher HIU power (500 W) was applied. According to the results of carbonyl content (Table 1), it was known that the protein oxidation at the level UVT group (500 W) reached the highest level. Therefore, the excess protein oxidation in the UVT group (500 W) might result in a decrease in the reactive SH content.

3.3. MPs secondary structure

The amide I band is one of the most informative Raman bands. The wavelength at the range of $1,600\text{--}1,700\text{ cm}^{-1}$ could reflect the secondary structural changes of proteins since different peaks correspond to different secondary structures [19]. The content of varying secondary structures of MPs is exhibited in Table 2. The HIU power, treatment time and their interaction had a significant influence on the α -helix content, β -sheet content and random coil content ($P < 0.05$), while the β -turn content was not significantly affected by those effects ($P > 0.05$). The VT treatment for 120 min caused a decrease in the α -helix content from 42.58% to 32.74%, whereas a raise in the β -sheet content from 17.23%

Table 1

Effects of different ultrasound power and treatment time on the carbonyl content, total and reactive sulfhydryl (SH) content of pork myofibrillar proteins.

	Treat time (min)	Ultrasound power (W)				SE ²	P-Values ¹		
		0	100	300	500		Power	Time	Time \times Power
Carbonyl group (nmol mg/ protein)	0	0.19 ^{ay}	0.19 ^{az}	0.19 ^{az}	0.20 ^{az}	0.067	<0.001	<0.001	0.0001
	60	0.27 ^{cx}	0.43 ^{by}	0.51 ^{aby}	0.56 ^{ay}				
	120	0.32 ^{dx}	0.56 ^{cx}	0.66 ^{bx}	0.77 ^{ax}				
Total SH content (nmol /mg protein)	0	84.72 ^{ax}	84.45 ^{ax}	84.83 ^{ax}	84.84 ^{ax}	2.26	<0.001	<0.001	0.0102
	60	82.08 ^{ay}	79.73 ^{ay}	75.74 ^{by}	73.65 ^{by}				
	120	80.17 ^{ay}	76.28 ^{abz}	72.75 ^{bcy}	71.44 ^{cy}				
Reactive SH content (nmol /mg protein)	0	21.71 ^{ay}	22.21 ^{ay}	22.01 ^{ay}	21.58 ^{ay}	1.25	<0.001	<0.001	0.0262
	60	22.84 ^{by}	23.88 ^{by}	27.00 ^{ax}	22.25 ^{by}				
	120	25.02 ^{bx}	27.99 ^{ax}	28.92 ^{ax}	25.28 ^{bx}				

³ a ~ d in the same row indicate a significant difference between ultrasound power ($P < 0.05$).

⁴ x ~ z in the same column indicate significant difference between treatment time ($P < 0.05$).

⁵ indexes at the 0 min express the initial value of myofibrillar proteins before treatment.

¹ P-Values indicate the level of significance including high-intensity ultrasound power, treatment time and their interaction.

² SE: standard error.

Table 2

Effects of different ultrasound power and treatment time on the secondary structures of pork myofibrillar proteins.

	Treat time (min)	Ultrasound power (W)				SE ²	P-Values ¹		
		0	100	300	500		Power	Time	Time × Power
α -Helix (%)	0	42.58 ^{ax}	42.27 ^{ax}	42.22 ^{ax}	42.94 ^{ax}	2.61	<0.001	<0.001	<0.001
	60	38.96 ^{ax}	30.36 ^{by}	19.93 ^{cy}	31.70 ^{by}				
	120	32.74 ^{ay}	26.95 ^{by}	18.05 ^{cy}	32.67 ^{ay}				
β -Sheet (%)	0	17.23 ^{ay}	18.46 ^{ay}	18.40 ^{ay}	17.45 ^{ay}	2.54	<0.001	<0.001	0.0052
	60	23.28 ^{bx}	24.89 ^{bx}	31.44 ^{ax}	23.51 ^{bx}				
	120	23.80 ^{bcx}	25.69 ^{bx}	32.97 ^{ax}	19.70 ^{cy}				
β -Turn (%)	0	17.72 ^{ax}	16.67 ^{ax}	15.90 ^{ax}	18.01 ^{ax}	3.22	0.803	0.076	0.985
	60	17.55 ^{ax}	18.58 ^{ax}	16.47 ^{ax}	18.30 ^{ax}				
	120	19.54 ^{ax}	20.14 ^{ax}	19.77 ^{ax}	19.65 ^{ax}				
Random coil (%)	0	22.48 ^{ax}	22.61 ^{axby}	23.47 ^{ay}	21.60 ^{ay}	2.81	0.0003	0.0005	0.0454
	60	20.21 ^{cx}	26.17 ^{bx}	32.16 ^{ax}	26.49 ^{bx}				
	120	23.92 ^{ax}	27.23 ^{ax}	29.21 ^{ax}	27.98 ^{ax}				

³a ~ d in the same row indicate a significant difference between ultrasound power ($P < 0.05$).⁴x ~ z in the same column indicate significant difference between treatment time ($P < 0.05$).⁵indexes at the 0 min express the initial value of myofibrillar proteins before treatment.¹ P-Values indicate the level of significance including high-intensity ultrasound power, treatment time and their interaction.² SE: standard error.

to 23.80% was observed ($P < 0.05$). However, no significant changes in the β -turn content and the random coil content were found ($P > 0.05$) compared with the native protein structure (0 min). As HIU power (100 W and 300 W) and treatment time were increased, the modifications in the secondary structure became more evident. Compared with the VT group, the α -helix content in the UVT groups (100 W and 300 W) was further decreased at each treatment time. Meanwhile, the β -sheet content was increased drastically after treated by UVT with 300 W ($P < 0.05$). In addition, the random coil content of all UVT groups was considerably increased at 60 min ($P < 0.05$). However, when the HIU power was enhanced to 500 W, the α -helix content was oppositely increased compared to that of HIU power with 300 W at each treatment time, whereas the β -sheet content (60 min and 120 min) and the random coil were decreased (60 min).

The change of secondary structure under the 100 W and 300 W indicated that appropriate HIU could promote the transformation of α -helix into β -sheet and random coil. Many reports have pointed that the reduction of α -helix regions and the construction of β -sheet facilitated the exposure of the internal active groups in the protein and promoted protein-protein connection, which was conducive to MPs gelation and emulsion stability [28]. The α -helix structure is deemed to be stabilized by the hydrogen bonds, which are formed by C=O and N-H in the protein [29]. The decrease of α -helix content in the study suggested that UVT treatment was able to disrupt hydrogen bonds. Similar results were observed by Li et al. [28] when researched the effects of single HIU treatment on the chicken MPs. However, the content of α -helix increased

when the high power UVT was applied (500 W), which might attribute to the refolding and aggregation of MPs [30].

3.4. MPs tertiary structure

The value of S_0 as an indicator refers to the content of hydrophobic groups distributed on the surface of proteins, which contacts with the aqueous polar environment [31]. The value of S_0 could indicate the changes in protein conformation and denaturation in the samples. As shown in Table 3, the HIU power, treatment time and their interaction all displayed apparent effects on the S_0 values ($P < 0.05$). The S_0 values of UVT groups (100 W and 300 W) were significantly increased compared with VT groups ($P < 0.05$) regardless of tumbling treatment time. In addition, the S_0 values reached the maximum in the UVT group with 300 W at 60 min. According to the previous study, Li et al. [28] demonstrated that ultrasonic cavitation could expose hydrophobic regions to the surface that were originally embedded within the MPs molecule. Additionally, Cao et al. [32] illustrated that protein oxidation exerted the effects to expose the initially buried hydrophobic groups to the protein surface. Therefore, the increase of the S_0 values in this work was possibly due to the combined impacts of ultrasonic cavitation and protein oxidation. However, compared with the UVT group (300 W), the S_0 values decreased slightly upon further UVT treatment (500 W) at 60 min and 120 min. Similarly, Zou et al. [21] confirmed that excessive HIU intensity decreased the S_0 values, which could be due to the refolding and the aggregation of proteins, thus reburied the hydrophobic groups.

Table 3Effects of different ultrasound power and treatment time on the surface hydrophobicity (S_0), particle size and solubility of pork myofibrillar proteins.

	Treat time (min)	Ultrasound power (W)				SE ²	P-Values ¹		
		0	100	300	500		Power	Time	Time × Power
Surface hydrophobicity (S_0)	0	1383.20 ^{ay}	1385.48 ^{ay}	1375.16 ^{az}	1357.25 ^{ax}	95.24	<0.001	<0.001	<0.001
	60	1499.52 ^{cx}	1681.74 ^{bx}	2056.57 ^{ax}	1487.41 ^{cx}				
	120	1551.85 ^{bx}	1717.46 ^{ax}	1834.44 ^{ay}	1446.00 ^{bx}				
Particle size (μ m)	0	1790.0 ^{ax}	1792.5 ^{ax}	1746.67 ^{ax}	1750.0 ^{ax}	102.99	<0.001	<0.001	<0.001
	60	865.95 ^{ay}	615.65 ^{cy}	402.42 ^{dz}	747.32 ^{bz}				
	120	817.73 ^{by}	344.14 ^{dz}	662.71 ^{cy}	1181.18 ^{ay}				
Solubility (%)	0	31.92 ^{az}	32.31 ^{az}	33.09 ^{ay}	32.81 ^{ax}	3.33	<0.001	<0.001	<0.001
	60	37.61 ^{cy}	42.17 ^{by}	48.43 ^{ax}	27.14 ^{dx}				
	120	43.29 ^{bx}	48.80 ^{abx}	52.22 ^{ax}	28.76 ^{cx}				

³a ~ d in the same row indicate a significant difference between ultrasound power ($P < 0.05$).⁴x ~ z in the same column indicate significant difference between treatment time ($P < 0.05$).⁵indexes at the 0 min express the initial value of myofibrillar proteins before treatment.¹ P-Values indicate the level of significance including high-intensity ultrasound power, treatment time and their interaction.² SE: standard error.

The tertiary structural change of MPs also can be investigated by the fluorescence of tryptophan/tyrosine residues due to intrinsic fluorescence chromophores from those aromatic amino acids [33]. As shown in Fig. 2, the maximum fluorescence intensity of the VT group (60 min) was slightly increased compared with the initial fluorescence intensity of native protein (untreated raw meat), accompanied by the maximum emission wavelength (λ_{\max}) red-shift from 342 to 344 nm. After UVT treatment at HIU powers of 100 W and 300 W, the maximum fluorescence intensity increased compared with the VT group. The maximum intensity in the spectrum was the UVT group (300 W), which was treated for 60 min and then followed by the same group treated for 120 min. The spectrum illustrated that UVT treatment could lead to further unfold and expose the previously buried hydrophobic groups of MPs compared with the VT treatment. However, at each treatment time, the fluorescence intensity of the UVT group (500 W) was decreased in comparison with the UVT group (300 W). In addition, with 60 min UVT (500 W) treatment, the λ_{\max} was blue-shifted to 342 nm. These results suggest that high power UVT treatment could induce MPs aggregation through the hydrophobic interactions, which is in accordance with the outcome of S_0 (Table 3).

3.5. Particle size

The aggregation behavior of MPs was estimated by particle size as shown in Table 3. The HIU power, treatment time and their interaction significantly affected the particle size ($P < 0.05$). At 60 min, the particle size of MPs in the VT group was apparently decreased compared with the MPs initial particle size at 0 min ($P < 0.05$), while no significant changes were found when the tumbling treatment time increased to 120 min ($P > 0.05$). As for the UVT groups, at 60 min, the particle size was declined from 615.65 μm (100 W) to 402.42 μm (300 W) and then increased to 747.32 μm (500 W). The particle size of all UVT groups was significantly smaller than that of the VT group ($P < 0.05$), while it tended to increase when HIU power increased to 500 W in comparison with the particle size under 300 W treatment. Similarly, at 120 min, the particle size obtained the minimum value under 100 W treatment. In contrast, it was considerably increased as the HIU power was further increased to 300 W and 500 W ($P < 0.05$). The effects of HIU on particle size were also observed by Li et al. [34]. They indicated that lower HIU power treatment decreased the particle size of sea cucumber gonad protein. The reduced particle size might be related to that the moderate ultrasound cavitation could break the protein agglomerates into smaller particles and dissociate the noncovalent forces through turbulence and shear force [8]. In

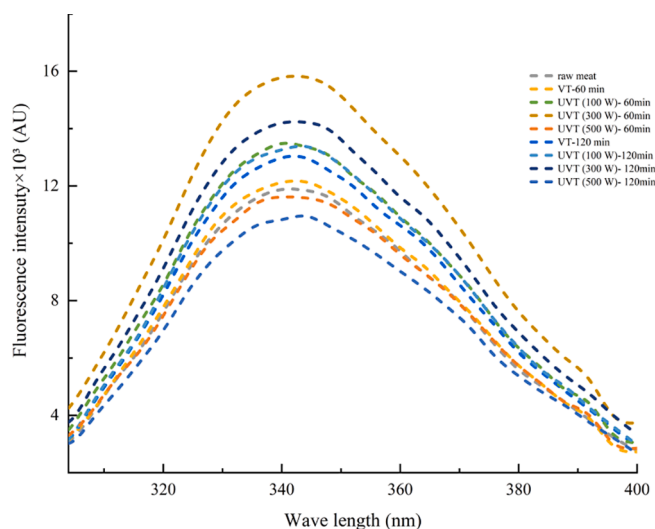


Fig. 2. Effects of different ultrasound power and treatment time on the intrinsic tryptophan emission fluorescence spectra of pork myofibrillar proteins.

contrast, the increased particle size might attribute to protein oxidation, which led to protein aggregation by disulfide bonds and cross-linking according to the results of SH content (Table 1) and the tertiary structure (Table 3 and Fig. 2) in the UVT group (500 W).

3.6. MPs solubility

Solubility is one of the most applicable indexes to reflect the denaturation, aggregation and oxidation of protein [35]. According to Table 3, the solubility was significantly affected by HIU power, treatment time and their interaction. Moreover, under the HIU power at 100 W and 300 W, the solubility was increased with the HIU power and treatment time compared with the VT group ($P < 0.05$). According to Zhang et al. [26], the ultrasonic cavitation could destroy the hydrogen bonds and hydrophobic interactions that existed in the aggregates of natural protein and lead to increased protein solubility. Amir et al. [8] also reported that HIU treatment could increase the solubility of protein by reducing the particle size of MPs. Our results are in accordance with the previous findings. The ultrasonic cavitation resulted from low power (100 W and 300 W) UVT treatment reduced the protein particle size, which was beneficial to the interaction of protein-water. In addition, the effects of cavitation combined with mild protein oxidation could unfold the structure of MPs, which further promoted the enhancement of solubility. Nevertheless, in the present work, when the HIU power was at 500 W, the solubility was lower than that of the VT group at each treatment time ($P < 0.05$). The results indicated that the excessive UVT (500 W) treatment may cause the refold of MPs structure and lead to a larger aggresome, thus resulting in the reduction of solubility. Zou et al. [21,25] found similar results that HIU treatment could decrease the protein solubility though negatively promoting protein assemble into agglomerates and generate cross-links. The solubility of MPs plays a key part in the functional properties of MPs. Since better solubility could ensure enough protein to form protein gel or emulsified with oil droplets, moderate UVT treatment (100 W and 300 W) may be further applied to improve protein functional properties.

4. Conclusions

The present study demonstrated that UVT treatment could induce protein oxidation and modify the physicochemical properties of MPs. The carbonyl content increased while the total SH content decreased with the HIU power being increased from 100 W to 500 W suggesting the increased levels of protein oxidation. The results of reactive SH content and the tertiary structure indicated that appropriate UVT treatment (100 W and 300 W) could unfold the MPs structure, and thus expose the SH groups and hydrophobic regions to the surface of the protein. Also, the orderly secondary structure was destroyed and the particle size was reduced by ultrasonic cavitation. While the solubility of MPs was improved especially treated by UVT treatment (100 W and 300 W). Overall, this study revealed that UVT treatment was able to induce protein oxidation. Under the moderate HIU power applied (100 W and 300 W), UVT treatment could change the structure of MPs and reduce the particle size to expand the protein-water interaction, thus positively improving the solubility.

CRedit authorship contribution statement

Ruyu Zhang: Conceptualization, Data curation, Methodology, Software, Formal analysis, Writing - original draft, Writing - review & editing, Investigation. **Lujuan Xing:** Resources, Investigation, Data curation. **Dacheng Kang:** Writing - review & editing. **Lei Zhou:** . **Lin Wang:** . **Wangang Zhang:** Supervision, Resources.

Declaration of Competing Interest

The authors declare that they have no known competing financial

interests or personal relationships that could have appeared to influence the work reported in this paper.

Acknowledgements

This research was supported by The State Key Research and Development Plan “Modern Food Processing and Food Storage and Transportation Technology and Equipment (2016YFD0400703; 2018YFD0400101); Jiangsu Agriculture Science and Technology Innovation Fund (CX(19)2018).

References

- [1] A.D. Alarcon-Rojo, H. Janacua, J.C. Rodriguez, L. Paniwnyk, T.J. Mason, Power ultrasound in meat processing, *Meat Sci.* 107 (2015) 86–93.
- [2] L. Zhou, J. Zhang, L. Xing, W. Zhang, Applications and effects of ultrasound assisted emulsification in the production of food emulsions: a review, *Trends Food Sci. Technol.* 110 (2021) 493–512.
- [3] D.C. Kang, W.G. Zhang, J.M. Lorenzo, X. Chen, Structural and functional modification of food proteins by high power ultrasound and its application in meat processing, *Crit. Rev. Food Sci. Nutr.* 1–20 (2020).
- [4] C. Ozuna, A. Puig, J.V. García-Pérez, A. Mulet, J.A. Cárcel, Influence of high intensity ultrasound application on mass transport, microstructure and textural properties of pork meat (*Longissimus dorsi*) brined at different NaCl concentrations, *J. Food Eng.* 119 (1) (2013) 84–93.
- [5] D.-C. Kang, A.-R. Wang, G.-H. Zhou, W.-G. Zhang, S.-M. Xu, G.-P. Guo, Power ultrasonic on mass transport of beef: effects of ultrasound intensity and NaCl concentration, *Innov. Food Sci. Emerg. Technol.* 35 (2016) 36–44.
- [6] J. Zhang, D.C. Kang, W.G. Zhang, J.M. Lorenzo, Recent advantage of interactions of protein-flavor in foods: perspective of theoretical models, protein properties and extrinsic factors, *Trends Food Sci. Technol.* 111 (2021) 405–425.
- [7] L. Jiang, J. Wang, Y. Li, Z. Wang, J. Liang, R. Wang, Y. Chen, W. Ma, B. Qi, M. Zhang, Effects of ultrasound on the structure and physical properties of black bean protein isolates, *Food Res. Int.* 62 (2014) 595–601.
- [8] A. Amiri, P. Sharifian, N. Soltanizadeh, Application of ultrasound treatment for improving the physicochemical, functional and rheological properties of myofibrillar proteins, *Int. J. Biol. Macromol.* 111 (2018) 139–147.
- [9] R.J. Krause, R.F. Plimpton, H.W. Ockerman, V.R. Cahill, Influence of tumbling and sodium tripolyphosphate on salt and nitrite distribution in porcine muscle, *J. Food Sci.* 43 (1) (1978) 190–192.
- [10] R.J. Krause, H.W. Ockerman, B. Krol, P.C. Moerman, R.F. Plimpton, Influence of tumbling, tumbling time, trim and sodium tripolyphosphate on quality and yield of cured hams, *J. Food Sci.* 43 (3) (1978) 853–855.
- [11] N.G. Marriott, P.P. Graham, J.W. Boling, W.F. Collins, Vacuum tumbling of dry-cured hams, *J. Anim. Sci.* 58 (1984) 1376–1381.
- [12] X. Chen, J. Luo, A.H. Lou, Y. Wang, D.W. Yang, Q.W.W. Shen, Duck breast muscle proteins, free fatty acids and volatile compounds as affected by curing methods, *Food Chem.* 338 (2021), 128138.
- [13] E. Demirok, N. Kolsarıcı, İ.T. Akoğlu, E. Özden, The effects of tumbling and sodium tripolyphosphate on the proteins of döner, *Meat Sci.* 89 (2) (2011) 154–159.
- [14] Y. Li, T. Feng, J.X. Sun, L.P. Guo, B.W. Wang, M. Huang, X.L. Xu, J.Y. Yu, H. Harvey, Physicochemical and microstructural attributes of marinated chicken breast influenced by breathing ultrasonic tumbling, *Ultrason. Sonochem.* 64 (2020), 105022.
- [15] M. Han, Y. Zhang, Y. Fei, X. Xu, G. Zhou, Effect of microbial transglutaminase on NMR relaxometry and microstructure of pork myofibrillar protein gel, *Eur. Food Res. Technol.* 228 (4) (2009) 665–670.
- [16] A.G. Gornall, C.J. Bardawill, M.M. David, Determination of serum proteins by means of the biuret reaction, *J. Biol. Chem.* 177 (2) (1949) 751–766.
- [17] Y.-P. Li, R. Liu, W.-G. Zhang, Q.-Q. Fu, N. Liu, G.-H. Zhou, Effect of nitric oxide on μ -calpain activation, protein proteolysis, and protein oxidation of pork during post-mortem aging, *J. Agric. Food Chem.* 62 (25) (2014) 5972–5977.
- [18] Q.-Q. Fu, R. Liu, W.-G. Zhang, Y.-P. Li, J. Wang, G.-H. Zhou, Effects of different packaging systems on beef tenderness through protein modifications, *Food Bioprocess Technol.* 8 (3) (2015) 580–588.
- [19] C.-Y. Zhou, C. Wang, J.-H. Cai, Y. Bai, X.-B. Yu, C.-B. Li, X.-L. Xu, G.-H. Zhou, J.-X. Cao, Evaluating the effect of protein modifications and water distribution on bitterness and adhesiveness of Jinhua ham, *Food Chem.* 293 (2019) 103–111.
- [20] L. Zhou, X. Feng, Y. Yang, Y. Chen, X. Tang, S. Wei, S. Li, Effects of high-speed shear homogenization on the emulsifying and structural properties of myofibrillar protein under low-fat conditions, *J. Sci. Food Agric.* 99 (14) (2019) 6500–6508.
- [21] Y.e. Zou, P. Xu, H. Wu, M. Zhang, Z. Sun, C. Sun, D. Wang, J. Cao, W. Xu, Effects of different ultrasound power on physicochemical property and functional performance of chicken actomyosin, *Int. J. Biol. Macromol.* 113 (2018) 640–647.
- [22] M. Dong, Y. Xu, Y. Zhang, M. Han, P. Wang, X. Xu, G. Zhou, Physicochemical and structural properties of myofibrillar proteins isolated from pale, soft, exudative (PSE)-like chicken breast meat: effects of pulsed electric field (PEF), *Innov. Food Sci. Emerg. Technol.* 59 (2020) 102277, <https://doi.org/10.1016/j.ifset.2019.102277>.
- [23] C. Li, Y.L. Xiong, J. Chen, Oxidation-induced unfolding facilitates myosin cross-linking in myofibrillar protein by microbial transglutaminase, *J. Agric. Food Chem.* 60 (32) (2012) 8020–8027.
- [24] M. Ashokkumar, The characterization of acoustic cavitation bubbles – a n overview, *Ultrason. Sonochem.* 18 (4) (2011) 864–872.
- [25] D.-C. Kang, Y.-h. Zou, Y.-P. Cheng, L.-J. Xing, G.-H. Zhou, W.-G. Zhang, Effects of power ultrasound on oxidation and structure of beef proteins during curing processing, *Ultrason. Sonochem.* 33 (2016) 47–53.
- [26] Z. Zhang, J.M. Regensteijn, P. Zhou, Y. Yang, Effects of high intensity ultrasound modification on physicochemical property and water in myofibrillar protein gel, *Ultrason. Sonochem.* 34 (2017) 960–967.
- [27] J.F. Pan, H.L. Lian, H. Jia, S.J. Li, R.Y. Hao, Y.J. Wang, X.N. Zhang, X.P. Dong, Ultrasound treatment modified the functional mode of gallic acid on properties of fish myofibrillar protein, *Food Chem.* 320 (2020), 126637.
- [28] K. Li, L. Fu, Y.Y. Zhao, S.W. Xue, P. Wang, X.L. Xu, Y.H. Bai, Use of high-intensity ultrasound to improve emulsifying properties of chicken myofibrillar protein and enhance the rheological properties and stability of the emulsion, *Food Hydrocolloid.* 98 (2020), 105275.
- [29] R. Tian, J. Feng, G. Huang, B. Tian, Y. Zhang, L. Jiang, X. Sui, Ultrasound driven conformational and physicochemical changes of soy protein hydrolysates, *Ultrason. Sonochem.* 68 (2020), 105202.
- [30] Y. Xu, R. Wang, H. Zhao, Y. Yin, X. Li, S. Yi, J. Li, Effect of heat treatment duration on the interaction between fish myosin and selected flavor compounds, *J. Sci. Food Agric.* 100 (12) (2020) 4457–4463.
- [31] H. Hu, J. Wu, E.C.Y. Li-Chan, L.e. Zhu, F. Zhang, X. Xu, G. Fan, L. Wang, X. Huang, S. Pan, Effects of ultrasound on structural and physical properties of soy protein isolate (SPI) dispersions, *Food Hydrocolloid.* 30 (2) (2013) 647–655.
- [32] Y. Cao, Y.L. Xiong, Chlorogenic acid-mediated gel formation of oxidatively stressed myofibrillar protein, *Food Chem.* 180 (2015) 235–243.
- [33] C.-Y. Zhou, J.-X. Cao, X.-B. Zhuang, Y. Bai, C.-B. Li, X.-L. Xu, G.-H. Zhou, Evaluation of the secondary structure and digestibility of myofibrillar proteins in cooked ham, *CyTA-J. Food.* 17 (1) (2019) 78–86.
- [34] H. Li, Y. Hu, X. Zhao, W. Wan, X. Du, B. Kong, X. Xia, Effects of different ultrasound powers on the structure and stability of protein from sea cucumber gonad, *LWT - Food Sci. Technol.* 137 (2021) 110403, <https://doi.org/10.1016/j.lwt.2020.110403>.
- [35] S. Liu, P. Zhao, J. Zhang, Q. Xu, Y. Ding, J. Liu, Physicochemical and functional properties of silver carp (*Hypophthalmichthys molitrix*) myofibrillar protein glycosylated with konjac oligo-glucomannan, *Food Hydrocolloid.* 67 (2017) 216–223.